Author(s): Papadakis, P.; Pakarinen, J.; Briscoe, A.D.; Cox, D.M.; Julin, R.; Auranen, K.; Grahn, T.; Greenlees, P.T.; Hadyńska-Klek, K.; Herzáň, A.; Herzberg, R.-D.; Jakobsson, U.; Juutinen, S.; Konki, J.; Leino, M.; Mistry, A.; O'Donnell, D.; Peura, P.; Rahkila, P.; Ruotsalainen, P.; Sandzelius, M.; Sarén, J.; Scholey, C.; Stoltze, S.; Sorri, J.; Uusitalo, J.; Wrzosek-Lipska, K.

Title: Direct observation of E0 transitions in 188Pb through in-beam spectroscopy

Year: 2024

Version: Published version

Please cite the original version:

Letter

Direct observation of $E0$ transitions in ^{188}Pb through in-beam spectroscopy

P. Papadakis [a,b], [ID],[*,1], J. Pakarinen [a], [ID],[**], A.D. Briscoe [a,2], D.M. Cox [a], R. Julin [a], K. Auranen [a],
T. Grahn [a], P.T. Greenlees [a], K. Hadyńska-Klek [c], A. Herzáň [a,d], R.-D. Herzberg [e], U. Jakobsson [a,3],
S. Juutinen [a], J. Konki [a], M. Leino [a], A. Mistry [e,4], D. O'Donnell [e,5], P. Peura [a], P. Rahkila [a],
P. Ruotsalainen [a], M. Sandzelius [a], J. Sarén [a], C. Scholey [a], S. Stoltze [a], J. Sorri [a,6], J. Uusitalo [a],
K. Wrzosek-Lipska [f,7]

[a] Accelerator Laboratory, Department of Physics, University of Jyväskylä, P.O. Box 35, FI-40014, University of Jyväskylä, Finland
[b] STFC Daresbury Laboratory, Daresbury, Warrington, WA4 4AD, UK
[c] Heavy Ion Laboratory, University of Warsaw, Warsaw, PL-02-093, Poland
[d] Institute of Physics, Slovak Academy of Sciences, 84511, Bratislava, Slovakia
[e] Department of Physics, Oliver Lodge Laboratory, University of Liverpool, P.O. Box 147, Liverpool, L69 7ZE, UK
[f] KU Leuven, Instituut voor Kern- en Stralingsfysica, B-3001, Leuven, Belgium

ARTICLE INFO

ABSTRACT

Competing configurations, assigned with three different shapes, are mixed at low angular momentum in the neutron-deficient ^{188}Pb nucleus. Here, we present a simultaneous conversion electron and γ-ray in-beam spectroscopic precision measurement employing the SAGE spectrometer. The level energy of the first excited state, 0_2^+, has been determined at 591(1) keV through direct measurement of conversion electrons. By using the intensity of the observed $0_2^+ \rightarrow 0_1^+$ transition to the ground state, the feeding of the 0_2^+ state has been determined for the first time, which suggests the 0_2^+ state is the head of the predominantly prolate band. The compositions of the $4_2^+ \rightarrow 4_1^+$ and $2_2^+ \rightarrow 2_1^+$ inter-band transitions have been determined, indicating configuration mixing between the bands.

1. Introduction

Shape coexistence and its role in the development of nuclear collectivity in atomic nuclei has been an intriguing topic for both theoretical and experimental studies for decades [1]. While nuclei at and near the magic neutron or proton numbers are spherical in their ground state, quadrupole deformed nuclei can be found all around the chart of nuclei [2]. These structures, arising from the interplay between single-particle motion, collectivity and pairing, can be assigned with different intrinsic configurations [1]. The first experimental evidence for triple-shape co-

existence was presented by Dracoulis et al. [3] when they associated three isomeric states in ^{188}Pb with different shapes. In the neutron-deficient Pb nuclei, competing structures intrude down in energy close to the ground states, best demonstrated in the unique case of the neutron $N = 104$ midshell nucleus ^{186}Pb, where each of the three lowest state possesses a different shape, namely spherical, prolate and oblate [4,5]. Laser spectroscopy experiments have confirmed the sphericity and small configuration mixing of the ground states of the even-mass $^{182-196}$Pb isotopes [6,7], whereas mixing of the excited low-spin states is predicted [8–10]. It has been experimentally demonstrated that mixing of the 2^+

---

states is strongest in the ^{188}Pb nucleus, which is also established as a crossing point for different structures at low excitation energy [11–13]. Since the 0_2^+ state in ^{188}Pb is the lowest excited state, the observed $E0(0_2^+ \rightarrow 0_1^+)$ intensity can be utilised as a tool to extract crucial information about the $E2$ transitions feeding the 0_2^+ state and therefore to probe the components of its wave function.

The discovery of intruder states in Pb nuclei was made by Van Duppen et al. [14], who observed the low-lying excited 0^+ states in even-mass $^{192-198}$Pb isotopes populated in the β-decay of odd-odd Bi nuclei. They associated these states with proton two-particle two-hole excitations across the $Z = 82$ shell closure and oblate shape. Further support for multiparticle-multihole configurations was gathered in α-decay fine-structure measurements of Po nuclei [15–19]. In-beam γ-ray experiments have confirmed the existence of deformed minima in the nuclear potential well by measuring rotational bands [20–22]. The first observation of excited states in ^{186}Pb and ^{188}Pb employing in-beam spectroscopy was made by Heese et al. [20]. They measured cascades of γ rays and based on similarities with yrast bands in ^{184,186}Hg isotones, associated them with a prolate-deformed rotational band. This was followed by the discovery of non-yrast structures and isomeric states associated with different macroscopic shapes in a comprehensive study of ^{188}Pb by Dracoulis et al. [23,12]. The existence of a prolate minimum was confirmed in the odd-mass ^{185}Pb nucleus by observation of a low-lying strongly coupled band [24]. The configuration mixing of the low-lying excited states in ^{186}Pb and ^{188}Pb has been probed in recoil-distance Doppler shift lifetime measurements [13,11], which concluded that the 2_1^+ state belongs to the yrast, predominantly prolate band. The development of collectivity of the $2_1^+ \rightarrow 0_1^+$ transitions has also been investigated in Coulomb excitation experiments employing radioactive ion beams [25,26].

None of the earlier experiments have been sensitive enough to measure transitions feeding the excited 0^+ band-head states in ^{188}Pb. The advent of the SAGE spectrometer [27] has allowed for the simultaneous in-beam measurement of both γ rays and conversion electrons with high efficiency, providing unparalleled sensitivity to probe $E0$ transitions in-beam as demonstrated by Ojala et al. [4]. In this Letter, we report on the first observation of a transition linking the intruder 0_2^+ band-head state with the non-yrast band in ^{188}Pb. The direct measurement of conversion electrons provides the most precise level energy for the 0_2^+ state to date, consistent with results reported in Refs. [16,18,19,28]. It is noteworthy, that our data do not provide evidence for the 0_3^+ state neither at 725 keV [28] nor 767 keV [17], which is in line with findings by Van de Vel et al. [19].

2. Experimental details

The experiment was performed in the Accelerator Laboratory of the University of Jyväskylä, Finland, employing the K130 cyclotron. The ^{188}Pb nuclei were produced via the ^{160}Dy(^{32}S,4n)^{188}Pb reaction with a beam energy of 165 MeV. Such an asymmetric reaction produces recoils with lower velocity and results in a smaller δ-electron yield compared to more symmetric reactions. These conditions are optimal for improving the performance of the prompt spectrometer. The ^{160}Dy target was a self-supporting metallic foil of thickness 500 μg/cm^2 giving rise to a cross section of 1.6(2) mb for the production of ^{188}Pb. Prompt γ rays and conversion electrons were detected at the target position of the RITU gas-filled recoil separator [29,30] by the SAGE spectrometer [27]. For γ-ray detection, SAGE employs 24 EUROGAM II four-fold segmented Clover [31] and 10 single-crystal (EUROGAM Phase I-type [32] and GASP-type [33]) Compton-suppressed Ge detectors. Internal conversion electrons were transported to a 90-fold annularly and radially segmented, 1-mm thick, Si detector by the magnetic field generated by applying 800 A to the solenoid coils of SAGE. The high rate of δ electrons, produced in interactions between the beam particles and atomic electrons in the target, were suppressed using -35 kV voltage on the SAGE high-voltage barrier.

Open ^{133}Ba and ^{207}Bi sources, and sealed ^{133}Ba and ^{152}Eu calibrated radioactive sources, were used for electron and γ-ray energy and absolute efficiency calibrations, respectively. Further information about the calibration process can be found in Ref. [27], where these are discussed in detail.

Fusion-evaporation residues (recoils hereafter) were separated from primary and scattered beam and other reaction products by RITU before being implanted into the double-sided silicon strip detectors (DSSDs) of the GREAT focal-plane spectrometer [34]. A transmission multiwire proportional counter (MWPC) upstream of the DSSDs, was used to obtain energy loss and timing information for the recoils. Any unwanted products which were not successfully suppressed by RITU were excluded from the data analysis by applying conditions on the energy loss in the MWPC and the time-of-flight between the MWPC and the DSSDs or through γ-γ and γ-e$^-$ coincidence gating. The effective beam-on-target time was approximately 129 hours, while the average beam current was 13 pnA.

Data were recorded using the triggerless total data readout system [35]. Spatial and temporal correlations of data were performed using the GRAIN software package [36], which was also used for data analysis together with the RADWARE software package [37].

3. Data analysis

Recoil-gated γ-ray and electron energy spectra collected during the experiment are shown in Fig. 1, where the most prominent peaks have been identified. The neighbouring nuclei which are most strongly present in the data are ^{189,190}Pb, ^{187,188,189}Tl and ^{186}Hg, with the relative production ratios shown in Fig. 1. In particular, transitions at 340 keV, 370 keV and 724 keV in the isobaric ^{188}Tl, overlapping with the yrast transitions in ^{188}Pb complicated the analysis of the data. In the conversion-electron spectrum in Fig. 1 the K- and L-conversion electrons associated with transitions in ^{188}Pb are labeled according to their corresponding transition energies.

A partial level scheme of ^{188}Pb including transitions relevant to the present work is also shown in Fig. 1. Corresponding K- and L-conversion electron energies for transitions with strong $E0$ components are marked in super- and subscript, respectively, next to the transition energy. Information extracted for relevant transitions from the present data are combined in Table 1 and Fig. 2 and discussed in the text. Information on other transitions observed in the present work are in agreement with published work [12] and are not included in Table 1.

The internal conversion coefficients (ICC) for the yrast transitions were extracted from the recoil-gated γ-ray and electron spectra where possible. Otherwise, ICCs were determined by gating on the $2_1^+ \rightarrow 0_1^+$ transition and comparing the measured γ rays and conversion electrons after correcting for absolute detection efficiencies. The direct comparison of the efficiency-corrected measured γ rays and internal conversion electrons is possible when they are produced under the same experimental and gating conditions. This technique was used to obtain all relevant results presented in this paper. In the case of the 251 keV $4_2^+ \rightarrow 4_1^+$ and 229 keV $2_2^+ \rightarrow 2_1^+$ inter-band transitions, ICCs were extracted by gating on the 340 keV $4_1^+ \rightarrow 2_1^+$ and 362 keV $4_2^+ \rightarrow 2_2^+$ intra-band transitions, respectively. In Fig. 2, ICCs from the K (α_K) and L (α_L) shells obtained from the present data are compared with values calculated with BrIcc [38], confirming the $E2$ multipole character of the yrast-band transitions up to the $10_1^+ \rightarrow 8_1^+$. Corresponding ICCs for $M1$ transitions would be two to five times larger.

For the inter-band $2_2^+ \rightarrow 2_1^+$ and $4_2^+ \rightarrow 4_1^+$ transitions, the presence of a strong $E0$ component becomes evident when comparing the measured ICCs with those calculated for pure $E2$ transitions (see Table 1). $M1$ components could partially explain the large ICCs, but as discussed e.g. in Ref. [12], $M1$ transitions are not permitted since the Clebsch-Gordan coefficient for an $J \rightarrow J$ $M1$ transition vanishes when both bands have $K = 0$. The statistics obtained was not sufficient to validate the multipole order of the interband transitions using angular correlations of γ rays.
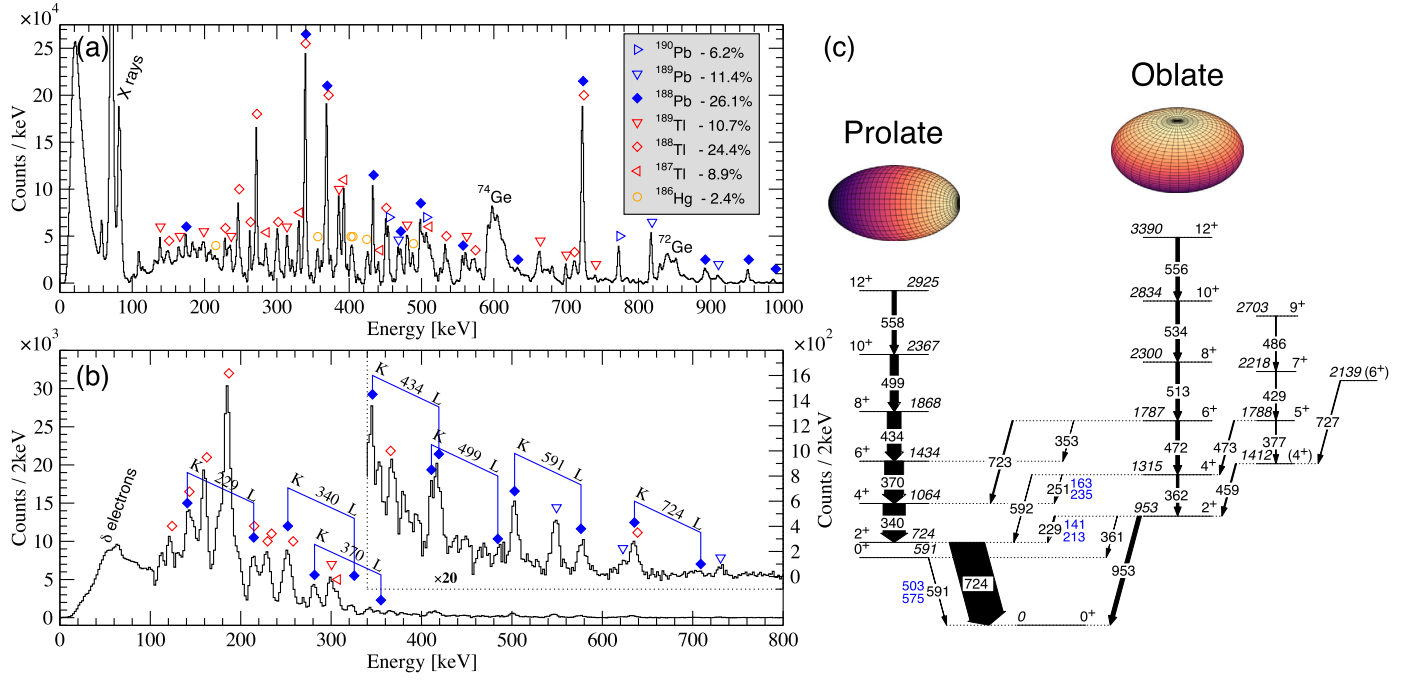
Fig. 1. Recoil-gated background subtracted γ-ray (a) and electron (b) energy spectra measured with the SAGE spectrometer. The origin of the most prominent peaks is indicated in the spectra. The strongest transitions in ^{188}Pb are labelled with the corresponding transition energy in the electron spectrum. The higher-energy electron peaks are shown in the inset of panel (b), where the y-axis has been expanded by a factor of 20 to allow for better visualisation. The relative production of nuclei composed in the experiment is shown in the inset of panel (a). In panel (c), a partial level scheme of ^{188}Pb with transitions relevant to the present work is shown. The two deformed rotational bands are labelled according to their predominant shape [12]. The widths of the arrows are relative to the total transition intensities. The corresponding K- and L-conversion electron energies for transitions with strong $E0$ components are marked in blue super- and subscript, respectively, next to the transition energy.

Table 1

Energies and intensities of γ rays and K- and L-conversion electrons for the transitions of interest obtained in the present work. Intensities are relative to that of the 724 keV $2_1^+ \to 0_1^+$ γ-ray transition. The α_K and α_L conversion coefficients are compared with values for pure $E2$ transitions calculated using BrIcc [38]. For some of the weaker transitions an upper limit was extracted for their intensity.

Transition $J_i^\pi \to J_f^\pi$	Transition energy [keV]	I_γ	$E_{e^-,K}$ [keV]	$I_{e^-,K}$	$E_{e^-,L}$ [keV]	$I_{e^-,L}$	α_K Meas	α_K Calc	α_L Meas	α_L Calc	$\alpha_{K/L}$ Meas	$\alpha_{K/L}$ Calc
$10_1^+ \to 8_1^+$	499(1)	251(14)	411(1)	5.5(8)	484(1)	2.2(5)	0.022(3)	0.0209(3)	0.009(2)	0.00653(1)	2.5(7)	3.19(7)
$8_1^+ \to 6_1^+$	434(1)	428(24)	346(1)	13.8(13)	419(1)	5.0(8)	0.032(2)	0.0281(4)	0.012(2)	0.01021(15)	2.8(5)	2.76(6)
$6_1^+ \to 4_1^+$	370(1)	575(32)	282(1)	24.4(2.4)	355(1)	10.2(1.1)	0.042(3)	0.0401(6)	0.018(2)	0.01758(25)	2.4(3)	2.25(5)
$4_1^+ \to 2_1^+$	340(1)	697(39)	252(1)	32.4(27)	325(1)	18.5(16)	0.046(3)	0.0486(7)	0.027(2)	0.02397(4)	1.8(2)	2.05(4)
$2_1^+ \to 0_2^+$	133(1)	<1.5	-	-	-	-	-	-	-	-	-	-
$2_1^+ \to 0_1^+$	724(1)	1000	636(1)	10.4(11)	708(1)	2.1(3)	0.010(1)	0.00981(14)	0.002(1)	0.00227(4)	5(9)	4.32(9)
$0_2^+ \to 0_1^+$	591(1)	-	503(1)	10.3(10)	575(1)	1.8(2)[a]	-	-	-	-	-	-
$6_2^+ \to 6_1^+$	353(1)	4(1)	-	-	-	-	-	-	-	-	-	-
$6_2^+ \to 4_2^+$	472(1)	103(6)	-	-	-	-	-	-	-	-	-	-
$6_2^+ \to 4_1^+$	724(1)	36(4)	-	-	-	-	-	-	-	-	-	-
$4_2^+ \to 4_1^+$	251(1)	12(1)	163(1)	14(3)	235(1)	<3.5	1.2(2)	0.0989(14)	<0.3	0.0759(11)	>4	1.30(3)
$4_2^+ \to 2_2^+$	362(1)	71(5)	-	-	-	-	-	-	-	-	-	-
$4_2^+ \to 2_1^+$	592(1)	82(6)	-	-	-	-	-	-	-	-	-	-
$2_2^+ \to 2_1^+$	229(1)	11(1)	141(1)	16(4)	213(1)	<4	1.5(3)	0.1228(18)	<0.4	0.1101(16)	>4	1.115(22)
$2_2^+ \to 0_2^+$	361(1)	3.4(12)	-	-	-	-	-	-	-	-	-	-
$2_2^+ \to 0_1^+$	953(1)	117(7)	-	-	-	-	-	-	-	-	-	-

[a] $I_{e^-,L}$ extracted using the $\alpha_{K/L_{I+II}}$ ratio of 5.79(5) for a pure $E0$ transition [38].

3.1. De-convolution of the high-energy recoil-gated electron energy spectrum

The high number of observed transitions in the recoil-gated spectra combined with the nature of internal conversion, where an electron from different atomic shells can be emitted in a transition, result in highly convoluted electron spectra with several overlapping peaks as presented in Fig. 3. In order to extract the $0_i^+ \to 0_f^+$ transition prop-erties, it was necessary to de-convolute the spectrum obtained. This was performed by identifying all transitions contributing to each in-dividual peak based on the observed γ-ray energy spectra and ICCs from literature. The de-convolution process in the energy range be-tween 460 and 840 keV, presented in Fig. 3 included more than 200 individual components. De-convolution was possible because of the si-multaneous detection of γ-rays and conversion electrons, allowed by SAGE.
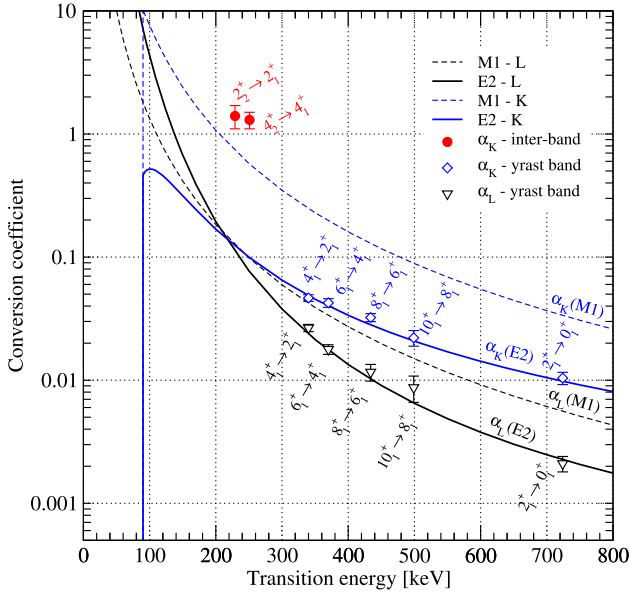
Fig. 2. Internal conversion coefficients obtained in the present work for the yrast- and inter-band transitions up to $J^\pi = 10^+$ and $J^\pi = 4^+$, respectively. Values are labelled according to the initial and final spins and parities. Calculated α_K and α_L values for pure $E2$ (solid) and $M1$ (dashed) transitions as a function of energy are plotted with black and blue lines, respectively, for comparison [38].
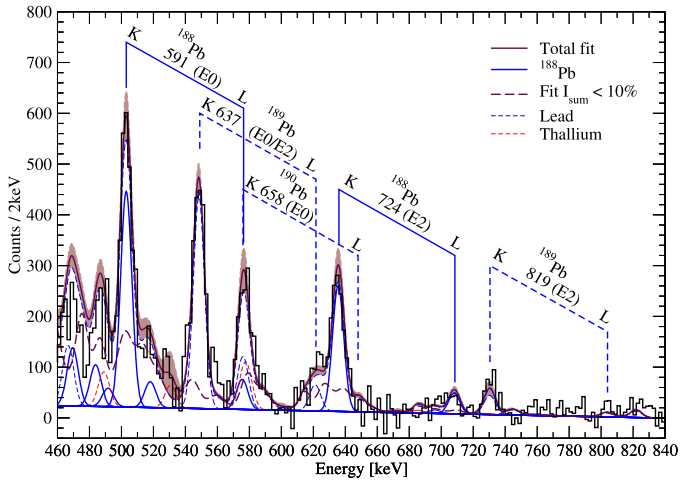

Fig. 3. De-convolution of the electron peaks in the region of 460-840 keV. The most prominent peaks have been marked and labelled with the transition energy and nucleus of origin. Transitions in ^{188}Pb are shown with the thick blue line. For clarity, only the transitions contributing 10% or more in each peak are plotted individually and the sum of all other transitions is plotted with a dashed maroon line. Transitions associated with ^{187,188,189}Tl are plotted with a dashed red line and with a dashed blue line those associated with ^{189,190}Pb. The thick maroon line is the sum of all components, including the ones not plotted here, while the brown band denotes errors of the total. The fitted peaks have been grouped according to the nucleus they belong to.

Using this de-convolution technique, the intensity of the 503 keV electrons, stemming from the K component of the 591 keV $0_2^+ \to 0_1^+$ transition [28], is identified as 10.3(10). After de-convoluting the peak at 575 keV, excess intensity of 4.9(9) could not be assigned to any transitions observed in the γ-ray energy spectra. This intensity can be assigned to the 591-L and 658-K electrons from the $0_2^+ \to 0_1^+$ transitions in ^{188}Pb and ^{190}Pb, respectively. Employing the $\alpha_{K/L_{I+II}}$ ratio of 5.79(5) for a pure $E0$ transition at 591 keV in Pb [38], we obtain an intensity of 1.8(2)
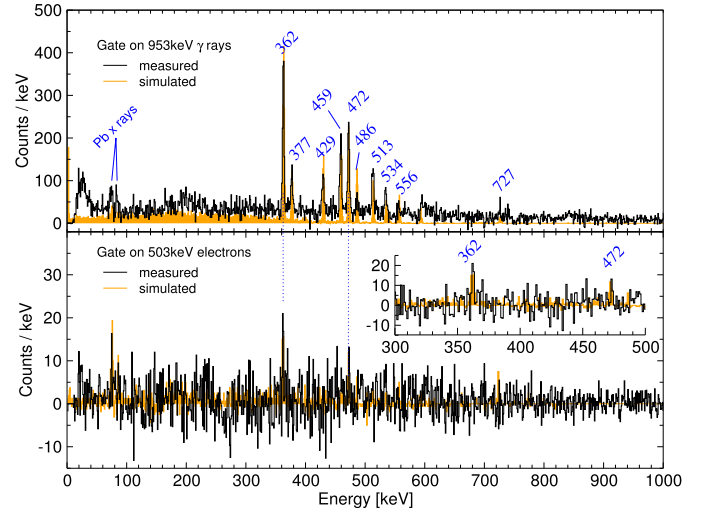

Fig. 4. Recoil-gated γ-ray energy spectrum gated on 953 keV γ rays (top) and 503 keV electrons (bottom). Dotted lines are marking expected peaks. Simulated spectra are filled in orange for comparison. The γ rays in coincidence with the 503 keV electrons place the 591 keV transition between the 0_2^+ and 0_1^+ states.

for the 575 keV (591-L) electrons. Therefore, the excess intensity of 3(1) units in the region of 575 keV is associated with the K component of the 658 keV $0_2^+ \to 0_1^+$ transition in ^{190}Pb. This corresponds to a 1.4(4)% feeding of the 0_2^+ state in ^{190}Pb with respect to the ground state, which is well in line with the corresponding value of 1.1(1)% extracted for ^{188}Pb.

The present data do not show evidence for the 0_3^+ state at 725 keV proposed by Le Coz et al. [28]. Through accurate de-convolution of the spectrum, all the observed electron intensity at 636 keV could be associated with known transitions, in particular the majority with the $2_1^+ \to 0_1^+$ 724 keV transition in ^{188}Pb.

3.2. Associating the 591 keV transition with the 0_2^+ state

In Fig. 4, γ-ray energy spectra gated on 953 keV γ rays (top) stemming from the $E2(2_2^+ \to 0_1^+)$ transition and 503 keV electrons (bottom) from the K-conversion electron line of the 591 keV $E0(0_2^+ \to 0_1^+)$ transition, are shown. The former reveals prominent peaks from transitions on top of the 2_2^+ state. From those the 362 and 472 keV peaks appear in the latter spectrum, while no yrast-band transitions are present, suggesting the feeding of the 0_2^+ state comes mainly from the non-yrast band on top of the 2_2^+ state.

It is also noteworthy that the $2_1^+ \to 0_1^+$ transition at 724 keV is not present in the 503 keV electron gate, ruling out the argument that the 503 keV electron peak originates from the $4_2^+ \to 2_1^+$ transition (see Fig. 1). Therefore, the majority of the detected electrons at 503 keV can be associated with the 591 keV transition to the ground state with a total intensity of 10.3(10). This observation confirms the direct observation of the $0_2^+ \to 0_1^+$ $E0$ transition by Le Coz et al. (591(2) keV) and is in agreement with the energies of 571(31) [16], 591(10) [18] and 588(4) keV [19] for the 0_2^+ state determined in α-decay fine-structure measurements. Experimental results have been verified with simulations. These simulations include a detailed representation of the SAGE spectrometer, and corrections on the energy of emitted electrons and γ rays based on reaction kinematics. Transitions in ^{188}Pb and other nuclei produced in the present work have been included in the simulation. A thorough description of these simulations will be presented in Ref. [39].

3.3. De-excitation paths from the 2_2^+ state

Recoil-gated γ-ray and electron energy spectra with a gate on 362 keV γ rays are shown in Fig. 5. Transitions associated with ^{188}Pb are labeled, while the 361 keV transition at the observational limit is
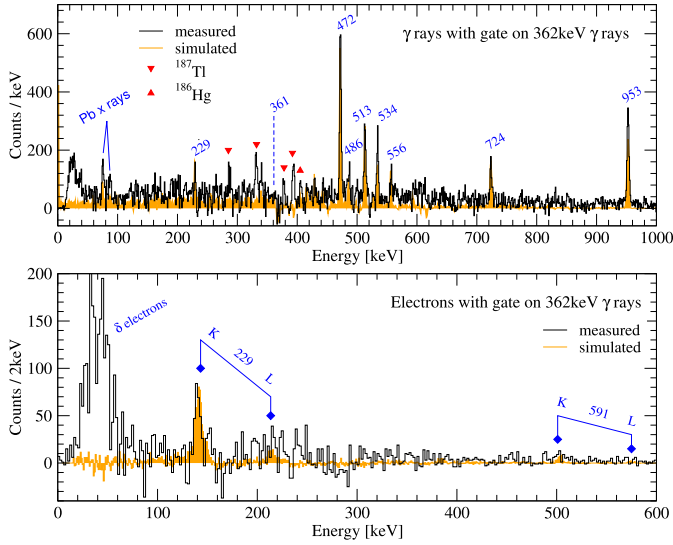
Fig. 5. Recoil-gated γ-ray (top) and electron (bottom) energy spectra with a gate on the 362 keV γ rays. Prominent γ-ray and the K- and L-conversion electron lines associated with ^{188}Pb have been labeled according to their transition energy. The γ rays associated with ^{187}Tl and ^{186}Hg contaminants are marked with red triangles. The 361 keV transition, which is at the observational limit has been marked with a dashed line. Simulated spectra are filled in orange for comparison.

Table 2

Relative B(E2) values extracted in the present work and absolute values obtained in the IBM calculations in Weisskopf units. The experimental values for transitions from the non-yrast band have been normalised to the one with the highest transition strength.

J^π_i	J^π_f	E_γ [keV]	B(E2)$_{Rel}$	B(E2)$_{IBM}$
6^+_2	6^+_1	353(1)	17(5)	75
	4^+_2	472(1)	100(13)	187
	4^+_1	724(1)	4.1(6)	1
4^+_2	4^+_1	251(1)	100(12)	109
	2^+_2	362(1)	95(10)	113
	2^+_1	592(1)	9.5(1.1)	4
2^+_2	2^+_1	229(1)	100(11)	98
	0^+_3	-	-	114
	0^+_2	361(1)	3.1(12)	33
	0^+_1	953(1)	0.8(1)	5
2^+_1	0^+_2	133(1)	< 90	95
	0^+_1	724(1)	7.5(30)[a]	13

[a] Absolute value extracted from lifetime measurements [42].

4. Discussion

4.1. Shape assignment of the 0^+_2 state

The 0^+_2 state at 591 keV is the first excited state in the ^{188}Pb nucleus and coexists with the spherical 0^+_1 ground state. The de-excitation paths, in particular the relative reduced transition probabilities ($B(E2)$ values from now on), from the predominantly prolate and oblate states provide invaluable information for the shape assignment of the excited 0^+ state. In Table 2, the relative $B(E2)$ values have been extracted from intensity balances and compared to those obtained using interacting boson model calculations (IBM) with configuration mixing [8]. In the neutron-deficient Pb region, the prolate intra-band $B(E2; J \to J-2)$ values are typically higher than those of the oblate band [8,10,13,40], whereas the inter-band $B(E2; J \to J)$ and $B(E2; J \to J-2)$ values depend strongly on the amount of configuration mixing.

If the 0^+_2 state was the head of the oblate band, the intra-band $B(E2; 2^+_2 \to 0^+_2)$ value should be at least that of the inter-band $2^+_2 \to 2^+_1$ transition, for example IBM calculations predict $B(E2; 2^+_2 \to 0^+_3)/B(E2; 2^+_2 \to 2^+_1) = 1.2$ (it is noteworthy, that in IBM the 0^+_3 state is assigned as oblate). For the $B(E2; 2^+_2 \to 0^+_2)/B(E2; 2^+_2 \to 2^+_1)$ ratio, IBM calculations give a value of 0.34, while in the present work we have obtained a value of 0.031(15). The closest comparison of the measured $B(E2)$ ratios involving inter-band transitions between the deformed 2^+ and 0^+ states can be made with ^{184}Hg, where the $B(E2; 2^+_2 \to 0^+_1)/B(E2; 2^+_2 \to 2^+_1)$ ratio is 0.044(14) [41]. It shows that the transition from the non-yrast 2^+ state to the yrast 2^+ state is similarly favoured over the transition to the yrast band-head 0^+ state (also noteworthy, that the spherical minimum is missing and the prolate-oblate potential energy minima are in different order in ^{184}Hg compared to those in ^{188}Pb). Consequently, since the $2^+_2 \to 0^+_2$ transition can only be assigned as an inter-band transition, our results suggest that the 0^+_2 state at 591 keV is the head of the predominantly prolate band. The earlier assignment of the 0^+_2 state with predominantly oblate shape was based on the reduced ^{192}Po α-decay widths [17,19]. Since the ground state of ^{192}Po is a mixture of different shape-driving configurations, reduced ^{192}Po α-decay widths are not conclusive probes for configuration assignment. It is also noteworthy, that the reduced α-decay width of 102(22) keV for the recently reassigned prolate 0^+_2 state in ^{186}Pb is very similar to the corresponding value of 90(18) keV extracted for the ^{192}Po α-decay to the 0^+_2 state in ^{188}Pb [19].

Since the feeding of the 0^+_2 state is mainly from the non-yrast band assigned with predominantly oblate shape, it is interesting to assess why the prolate intra-band $2^+_1 \to 0^+_2$ transition remained unobserved. The non-observation of the yrast-band transitions at 340 keV and 370 keV in Fig. 4 (bottom) renders a strict intensity limit of $I_{tot}(E2; 2^+_1 \to 0^+_2) < 4.5$

marked with a dashed line. The much higher intensity of the 229 keV K-electron peak in the bottom spectrum is a clear indication of the highly converted nature of this transition. This gate was used for the calculation of ICCs for the $2^+_2 \to 2^+_1$ transition. Simulated spectra are shown in orange. Apart from the low-energy δ-electron background, which is challenging to simulate, and contaminant transitions in the γ-ray energy spectrum due to the ideal simulation conditions, the simulated spectra strongly support our findings. Due to insufficient statistics for the 229 keV γ rays after the gate, the γ-ray intensity was extracted employing the known $\frac{I_{\gamma,953}}{I_{\gamma,229}}$ branching ratio [12] and γ rays measured for the 953 keV $2^+_2 \to 0^+_1$ transition.

It is noteworthy that no corresponding γ-ray transition at 591 keV has been observed in the 362 keV-gated γ-ray spectrum. In particular, if the electrons at 503 keV belonged to a 591 keV transition of $M1$ or $E2$ character then in the 362 keV-gated spectra we should observe 2500(500) or 10000(2000) γ rays, respectively, which is not the case.

Consequently, a weak cascade doublet, comprising the $4^+_2 \to 2^+_2$ and $2^+_2 \to 0^+_2$ transitions at 362 keV and 361 keV, respectively, is expected. Regardless of extensive efforts, the $2^+_2 \to 0^+_2$ transition has gone unobserved in an earlier experiment by Dracoulis et al. [12]. However, an upper limit of $I_\gamma < 6$, in the units of Table 1, was extracted from their data [23]. The recoil-gated electron energy spectrum with a gate on 362 keV γ rays shown in the bottom of Fig. 5 allows for extracting the intensity of $I_\gamma = 3.4(12)$ for the 361 keV $2^+_2 \to 0^+_2$ transition, which agrees with Dracoulis' observation. This was possible, since the intensity of the 503 keV electrons in the spectrum can be directly associated to the intensity of the 361 keV gating transition. It is important to note, that this intensity is about twice that of the 591 keV $0^+_2 \to 0^+_1$ transition observed in the same gate. Further evidence for the existence of the 361 keV $2^+_2 \to 0^+_2$ transition can be obtained from Fig. 4. The intensity ratio for the 362 keV/472 keV peaks when gating on the $2^+_2 \to 0^+_1$ transition (top) is 1.3(1), whereas gating on the $0^+_2 \to 0^+_1$ transition (bottom) returns a value of 2.8(12). As discussed above, this indicates that the peak at 362 keV is about twice as intense as the peak at 472 keV, which is well in line with our interpretation that the 362 keV peak is a doublet.
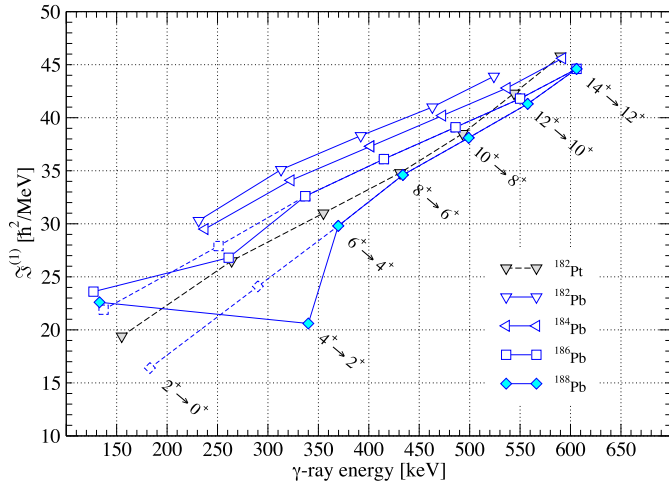
Fig. 6. Kinematic moment of inertia $\mathcal{J}^{(1)}$ as a function of γ-ray energy for the prolate bands in the neutron-deficient Pb nuclei [4,12,45–47]. A curve for the yrast band in ^{182}Pt is shown as a reference for an unperturbed prolate band in the region [48]. Dashed extensions to the ^{186}Pb and ^{188}Pb curves present cases where +10 keV and +50 keV have been added to the 2_1^+ level energies, respectively.

and further $I_\gamma(E2; 2_1^+ \to 0_2^+) < 1.5$. Together with the adopted lifetime of 8.5(35) ps for the 2_1^+ state [42], an upper limit of B(E2;$2_1^+ \to 0_2^+$) < 90 W.u. can be deduced. This shows that the $2_1^+ \to 0_2^+$ transition can still be a collective intra-band transition from a mixed 2_1^+ state.

The level energy systematics and lifetime measurements reveal that the mixing between the 2^+ states is strong especially in ^{188}Pb [8,11, 13,43]. This mixing can result in $E2$ transition strengths between the low-spin states that are much smaller than those for intra-band transitions at high spin. However, the difference between the measured $B(E2; 2_2^+ \to 0_1^+)/B(E2; 2_2^+ \to 2_1^+)$ and $B(E2; 2_2^+ \to 0_2^+)/B(E2; 2_2^+ \to 2_1^+)$ ratios to those obtained with IBM suggests that the mixing of the 0^+ states appears too strong in the IBM calculations. In the IBM calculations, the 2_1^+ [2_2^+] state is a mixture of configurations assigned with spherical, prolate and oblate shapes with admixtures of 26% [20%], 61% [30%] and 13% [50%] weights in their wave functions, respectively [8], whereas approximately 50% prolate admixture in the 2_1^+ state has been extracted from the $B(E2)$ values obtained in lifetime experiments [11,13]. The earlier IBM calculation with less experimental data employed in the normalisation showed very similar configuration mixing as stated above.

The assignment of the 0_2^+ state with predominantly prolate shape allows for extending the kinematic moment of inertia plot as presented in Fig. 6. Together with the recent assignment of the corresponding state in the ^{186}Pb nucleus [4], they are the only Pb isotopes where the level energy of the prolate band-head is determined employing in-beam spectroscopy. Deviation of the points related to the $4_1^+ \to 2_1^+$ and $2_1^+ \to 0_1^+$ transitions in ^{186}Pb and ^{188}Pb from the smooth curve can be explained by mixing of the 2^+ states. The level energies of the excited 0^+ states are affected only little by weak mixing with the spherical 0_1^+ ground state [8]. Therefore, in Fig. 6 the $2_1^+ \to 0_1^+$ transition energies in ^{186}Pb and ^{188}Pb appear lower and $\mathcal{J}^{(1)}$ values higher than those for an unperturbed rotational band, like the yrast band in ^{182}Pt. Indeed, this is also evident in Fig. 6. The level energies of the unperturbed 2_1^+ states in ^{186}Pb and ^{188}Pb can be estimated by correcting the 2_1^+ level energies to match with the smooth behaviour of the yrast band in ^{182}Pt. In Fig. 6, dashed extensions to the ^{186}Pb and ^{188}Pb curves correspond to +10 keV and +50 keV corrections, respectively. Using equations derived within the two-state mixing model (see e.g. Ref. [44]), values for mixing matrix element V_2 of 95 keV and mixing amplitude a^2 of 0.8 (80/20 mixing) can be obtained for the 2_1^+ state in ^{188}Pb.

Finally, the assignment of the 0_2^+ state with predominantly prolate shape is supported by theoretical calculations reported in Refs. [8,9,40,49], but it also challenges predictions claiming that the lowest deformed potential energy minimum in ^{188}Pb is oblate [10,50–52]. It should be noted, that competition between prolate and oblate minima is present in all of these calculations and for example the very early work by May et al. did not clearly assign which one is lower in energy [53]. Moreover, Refs. [10,51] do not reproduce the experimentally determined ordering of the prolate and oblate rotational bands in ^{188}Pb. When placing the predominantly prolate 0_2^+ state in ^{188}Pb in the level energy systematics plot of Ref. [4], the parabolic behaviour of the 0_2^+ level energies in ^{184,186,188}Pb is evident and it follows the similar trend established in Hg isotopes and for the higher spin prolate intruder states in the Pb isotopes [21].

4.2. Assessing the monopole strength of the inter-band transitions

As demonstrated in Fig. 2, the ICC values obtained for the $2_2^+ \to 2_1^+$ and $4_2^+ \to 4_1^+$ transitions can only be explained by the presence of strong $E0$ components, which in turn can arise from shape mixing. For a prolate (oblate) band, the quadrupole deformation value of $|\beta_2| = 0.29(5)$ ($|\beta_2| = 0.17(3)$) has been extracted from lifetime measurements performed in this region [13]. Adopting these values and 80/20 mixing, $\rho^2 = 190 \times 10^{-3}$ can be obtained for an oblate-prolate $E0$ transition in Pb nuclei [54]. Using this value for the $E0$-component and pure $E2$ character for the γ-ray emission component of the $2_2^+ \to 2_1^+$ transition, the present branching ratio of Table 1 results in a $B(E2)$ value of 5.3 W.u. for the $2_2^+ \to 0_1^+$ transition. This is close to the configuration-changing $2^+ \to 0^+$ transitions in Pb and Hg nuclei in this region [13,41,55]. However, that would mean a non-physically large $B(E2; 2_2^+ \to 2_1^+)$ value of ~ 630 W.u., suggesting the mixing of the two shapes is overestimated, or a presence of multipole mixing $\delta(E2/M1)$ in this transition. A relatively small $M1$ component would strongly reduce the $B(E2)$ value without much reduction in the $E0$ component. Such an $M1$ component has been proposed to be a result from a mixture between the oblate and γ band [12]. Three-level mixing calculations reveal that a spherical component is present in the lowest 2^+ states of ^{188}Pb [8,11,12]. Such a third component could lead to a drastic reduction of the ρ^2 value due to destructive interference in the mixing of shape-coexisting structures [56].

The monopole strength of the $4_2^+ \to 4_1^+$ transition can be assessed similarly. Since the relative $B(E2)$ values from the 4_2^+ state are fairly close to those obtained in the IBM calculations, using the $B(E2; 4_2^+ \to 2_2^+)$ value of 113 W.u. is justified. The $\rho^2 = 50 \times 10^{-3}$ value obtained corresponds to 5/95 prolate-oblate mixing. The small deviation of the point corresponding to the $6_1^+ \to 4_1^+$ transition in Fig. 6 from the smooth curve also supports the argument that the mixing of the 4^+ states is smaller than that of the 2^+ states.

5. Conclusions

$E0$ transitions in the neutron-deficient ^{188}Pb nucleus have been measured in a γ-ray-conversion electron cross-coincidence experiment. The level energy of the first excited 0^+ state has been confirmed and measured with high accuracy. Moreover, the conversion electron components of the $J^+ \to J^+$ interband transitions have been determined in a direct measurement. These findings have been validated via extensive Geant4 simulations that include level schemes of twelve other nuclei produced in the same reaction.

The present work clarifies the low-spin level structure of ^{188}Pb reported in literature and assigns the first excited 0^+ state with predominantly prolate shape. In particular, our data provide no evidence for the second excited 0^+ state at 725 keV or 767 keV that have been reported in in-beam electron spectroscopy and α-decay fine structure experiments, respectively.

The results obtained provide valuable information for the analysis of complementary data, such as Coulomb excitation studies employing radioactive ion beams. The recently developed SPEDE spectrometer [57] will allow for extraction of matrix elements along the deformed bands in Coulomb excitation measurements at HIE-ISOLDE. Complementarily, the lifetimes of the excited 0^+ states, although very challenging, could be probed employing the recoil-shadow electron spectroscopy technique. The 0^+ state with predominantly oblate shape and the predominantly spherical 2^+ state remain to be discovered. The potential of transfer reaction measurements, which could also shed light on the intrinsic structure of the intruder states in this region, is noted.

Declaration of competing interest

The authors declare that they have no known competing financial interests or personal relationships that could have appeared to influence the work reported in this paper.

Data availability

Acknowledgements

References

[1] K. Heyde, J.L. Wood, Rev. Mod. Phys. 83 (4) (2011) 1467–1521, https://doi.org/10.1103/RevModPhys.83.1467.

[2] P. Möller, A.J. Sierk, R. Bengtsson, H. Sagawa, T. Ichikawa, Phys. Rev. Lett. 103 (21) (2009) 6, https://doi.org/10.1103/PhysRevLett.103.212501.

[3] G.D. Dracoulis, A.P. Byrne, A.M. Baxter, P.M. Davidson, T. Kibédi, T.R. McGoram, R.A. Bark, S.M. Mullins, Phys. Rev. C 60 (1999) 014303, https://doi.org/10.1103/PhysRevC.60.014303.

[4] J. Ojala, J. Pakarinen, P. Papadakis, J. Sorri, M. Sandzelius, D.M. Cox, K. Auranen, H. Badran, P.J. Davies, T. Grahn, P.T. Greenlees, J. Henderson, A. Herzáň, R.-D. Herzberg, J. Hilton, U. Jakobsson, D.G. Jenkins, D.T. Joss, R. Julin, S. Juutinen, T. Kibédi, J. Konki, G.J. Lane, M. Leino, J. Liimatainen, C.G. McPeake, O. Neuvonen, R.D. Page, E. Parr, J. Partanen, P. Peura, P. Rahkila, J. Revill, P. Ruotsalainen, J. Sarén, C. Scholey, S. Stolze, J. Uusitalo, A. Ward, R. Wadsworth, Commun. Phys. 5 (1) (2022) 213, https://doi.org/10.1038/s42005-022-00990-4.

[5] A.N. Andreyev, M. Huyse, P. Van Duppen, L. Weissman, D. Ackermann, J. Gerl, F.P. Hessberger, S. Hofmann, A. Kleinböhl, G. Münzenberg, S. Reshitko, C. Schlegel, H. Schaffner, P. Cagarda, M. Matos, S. Saro, A. Keenan, C. Moore, C.D. O'Leary, R.D. Page, M. Taylor, H. Kettunen, M. Leino, A. Lavrentiev, R. Wyss, K. Heyde, Nature 405 (6785) (2000) 430–433, https://doi.org/10.1038/35013012.

[6] U. Dinger, J. Eberz, G. Huber, R. Menges, S. Schröder, R. Kirchner, O. Klepper, T. Kühl, D. Marx, G.D. Sprouse, Z. Physik A - Atomic Nuclei 328 (2) (1987) 253–254, https://doi.org/10.1007/BF01290669.

[7] H. De Witte, A.N. Andreyev, N. Barré, M. Bender, T.E. Cocolios, S. Dean, D. Fedorov, V.N. Fedoseyev, L.M. Fraile, S. Franchoo, V. Hellemans, P.H. Heenen, K. Heyde, G. Huber, M. Huyse, H. Jeppessen, U. Köster, P. Kunz, S.R. Lesher, B.A. Marsh, I. Mukha, B. Roussière, J. Sauvage, M. Seliverstov, I. Stefanescu, E. Tengborn, K. Van de Vel, J. Van de Walle, P. Van Duppen, Yu. Volkov, Phys. Rev. Lett. 98 (11) (2007) 112502, https://doi.org/10.1103/PhysRevLett.98.112502.

[8] V. Hellemans, S. De Baerdemacker, K. Heyde, Phys. Rev. C 77 (2008) 064324, https://doi.org/10.1103/PhysRevC.77.064324.

[9] J.M. Yao, M. Bender, P.-H. Heenen, Phys. Rev. C 87 (2013) 034322, https://doi.org/10.1103/PhysRevC.87.034322.

[10] K. Nomura, R. Rodríguez-Guzmán, L.M. Robledo, N. Shimizu, Phys. Rev. C 86 (2012) 034322, https://doi.org/10.1103/PhysRevC.86.034322.

[11] A. Dewald, R. Peusquens, B. Saha, P. von Brentano, A. Fitzler, T. Klug, I. Wiedenhöver, M. Carpenter, A. Heinz, R.V.F. Janssens, F.G. Kondev, C.J. Lister, D. Seweryniak, K. Abu Saleem, R. Krücken, J.R. Cooper, C.J. Barton, K. Zyromski, C.W. Beausang, Z. Wang, P. Petkov, A.M. Oros-Peusquens, U. Garg, S. Zhu, Phys. Rev. C 68 (2003) 034314, https://doi.org/10.1103/PhysRevC.68.034314.

[12] G.D. Dracoulis, G.J. Lane, A.P. Byrne, T. Kibédi, A.M. Baxter, A.O. Macchiavèlli, P. Fallon, R.M. Clark, Phys. Rev. C 69 (2004) 054318, https://doi.org/10.1103/PhysRevC.69.054318.

[13] T. Grahn, A. Dewald, O. Möller, R. Julin, C.W. Beausang, S. Christen, I.G. Darby, S. Eeckhaudt, P.T. Greenlees, A. Görgen, K. Helariutta, J. Jolie, P. Jones, S. Juutinen, H. Kettunen, T. Kröll, R. Krücken, Y.Le Coz, M. Leino, A.-P. Leppänen, P. Maierbeck, D.A. Meyer, B. Melon, P. Nieminen, M. Nyman, R.D. Page, J. Pakarinen, P. Petkov, P. Rahkila, B. Saha, M. Sandzelius, J. Sarén, C. Scholey, J. Uusitalo, Phys. Rev. Lett. 97 (6) (2006) 062501, https://doi.org/10.1103/PhysRevLett.97.062501.

[14] P. Van Duppen, E. Coenen, K. Deneffe, M. Huyse, K. Heyde, P. Van Isacker, Phys. Rev. Lett. 52 (22) (1984) 1974–1977, https://doi.org/10.1103/PhysRevLett.52.1974.

[15] P. Van Duppen, E. Coenen, K. Deneffe, M. Huyse, J.L. Wood, Phys. Lett. B 154 (1985) 354–357, https://doi.org/10.1016/0370-2693(85)90408-3.

[16] N. Bijnens, I. Ahmad, A.N. Andreyev, J.C. Batchelder, C.R. Bingham, D. Blumenthal, B.C. Busse, X.S. Chen, L.F. Conticchio, C.N. Davids, M. Huyse, R.V.F. Janssens, P. Mantica, H. Penttila, W. Reviol, D. Seweryniak, P. Van Duppen, W.B. Walters, J. Wauters, B.E. Zimmerman, Z. Phys. A, Hadrons Nucl. 356 (1) (1996) 3–4, https://doi.org/10.1007/s002180050137.

[17] R.G. Allatt, R.D. Page, M. Leino, T. Enqvist, K. Eskola, P.T. Greenlees, P. Jones, R. Julin, P. Kuusiniemi, W.H. Trzaska, J. Uusitalo, Phys. Lett. B 437 (1–2) (1998) 29–34, https://doi.org/10.1016/S0370-2693(98)00939-3.

[18] A.N. Andreyev, N. Bijnens, M. Huyse, P. Van Duppen, M. Leino, T. Enqvist, P. Kuusiniemi, W. Trzaska, J. Uusitalo, N. Fotiades, J.A. Cizewski, M.P. McNabb, K.Y. Ding, C.N. Davids, R.V.F. Janssens, D. Seweryniak, M.P. Carpenter, H. Amro, P. Decrock, P. Reiter, D. Nisius, L.T. Brown, S. Fischer, T. Lauritsen, J. Wauters, C.R. Bingham, L.F. Conticchio, J. Phys. G, Nucl. Part. Phys. 25 (1999) 835–837, https://doi.org/10.1088/0954-3899/25/4/049.

[19] K. Van de Vel, A.N. Andreyev, D. Ackermann, H.J. Boardman, P. Cagarda, J. Gerl, F.P. Heßberger, S. Hofmann, M. Huyse, D. Karlgren, I. Kojouharov, M. Leino, B. Lommel, G. Münzenberg, C. Moore, R.D. Page, S. Saro, P. Van Duppen, R. Wyss, Phys. Rev. C 68 (2003) 054311, https://doi.org/10.1103/PhysRevC.68.054311.

[20] J. Heese, K.H. Maier, H. Grawe, J. Grebosz, H. Kluge, W. Meczynski, M. Schramm, R. Schubart, K. Spohr, J. Styczen, Phys. Lett. B 302 (4) (1993) 390–395, https://doi.org/10.1016/0370-2693(93)90415-E.

[21] R. Julin, K. Helariutta, M. Muikku, J. Phys. G, Nucl. Part. Phys. 27 (5) (2001) R109–R139, https://doi.org/10.1088/0954-3899/27/7/201.

[22] R. Julin, T. Grahn, J. Pakarinen, P. Rahkila, J. Phys. G, Nucl. Part. Phys. 43 (2) (2016) 024004, https://doi.org/10.1088/0954-3899/43/2/024004.

[23] G.D. Dracoulis, Private communication, 2013.

[24] J. Pakarinen, A.N. Andreyev, R. Julin, S. Juutinen, S. Antalic, L. Bianco, I.G. Darby, S. Eeckhaudt, T. Grahn, P.T. Greenlees, D.G. Jenkins, P. Jones, P. Joshi, H. Kettunen, M. Leino, A.-P. Leppänen, P. Nieminen, M. Nyman, R.D. Page, J. Perkowski, P.M. Raddon, P. Rahkila, D. Rostron, J. Sarén, C. Scholey, J. Sorri, B. Streicher, J. Uusitalo, K. Van de Vel, M. Venhart, R. Wadsworth, D.R. Wiseman, Phys. Rev. C 80 (2009) 031303, https://doi.org/10.1103/PhysRevC.80.031303.

[25] J. Pakarinen, T. Grahn, L.P. Gaffney, A. Algora, C. Bauer, A. Blazhev, N. Bree, T.E. Cocolios, H.De Witte, J. Diriken, P. Fernier, K. Hadyńska-Klęk, A. Herzáň, M. Huyse, J. Iwanicki, U. Jakobsson, D. Jenkins, N. Kesteloot, J. Konki, B. Lannoo, P. Papadakis, P. Peura, P. Rahkila, G. Rainovski, E. Rapisarda, P. Reiter, S. Sambi, M. Scheck, B. Seibeck, M. Seidlitz, T. Stora, P.V. Duppen, N. Warr, F. Wenander, M.J. Vermeulen, D. Voulot, K. Wrzosek-Lipska, M. Zielińska, J. Phys. G, Nucl. Part. Phys. 44 (6) (2017) 064009, https://doi.org/10.1088/1361-6471/aa6753.

[26] J. Pakarinen, T. Grahn, A. Algora, N. Bree, T.E. Cocolios, J. Diriken, P. Fernier, L.P. Gaffney, K. Hadyńska-Klęk, A. Herzáň, J. Iwanicki, U. Jakobsson, D. Jenkins, N. Kesteloot, J. Konki, B. Lannoo, P. Papadakis, P. Peura, P. Rahkila, G. Rainovski, E. Rapisarda, S. Sambi, M. Scheck, M. Seidlitz, T. Stora, P. Van Duppen, N. Warr, F. Wenander, M.J. Vermeulen, D. Voulot, K. Wrzosek-Lipska, M. Zielińska, JPS Conf. Proc. 6 (2015), https://doi.org/10.7566/JPSCP.6.020011.

[27] J. Pakarinen, P. Papadakis, J. Sorri, R.-D. Herzberg, P.T. Greenlees, P.A. Butler, P.J. Coleman-Smith, D.M. Cox, J.R. Cresswell, P. Jones, R. Julin, J. Konki, I.H. Lazarus, S.C. Letts, A. Mistry, R.D. Page, E. Parr, V.F.E. Pucknell, P. Rahkila, J. Sampson, M. Sandzelius, D.A. Seddon, J. Simpson, J. Thornhill, D. Wells, Eur. Phys. J. A 50 (3) (2014) 53, https://doi.org/10.1140/epja/i2014-14053-6.

[28] Y. Le Coz, F. Becker, H. Kankaanpää, W. Korten, E. Mergel, P.A. Butler, J.F.C. Cocks, O. Dorvaux, D. Hawcroft, K. Helariutta, R.-D. Herzberg, M. Houry, H. Hübel, P. Jones, R. Julin, S. Juutinen, H. Kettunen, P. Kuusiniemi, M. Leino, R. Lucas, M. Muikku, P. Nieminen, P. Rahkila, D. Rossbach, A. Savelius, Ch. Theisen, EPJ direct 1 (1) (2000) 1–6, https://doi.org/10.1007/s1010599a0003.

[29] M. Leino, J. Äystö, T. Enqvist, P. Heikkinen, A. Jokinen, M. Nurmia, A. Ostrowski, W.H. Trzaska, J. Uusitalo, K. Eskola, P. Armbruster, V. Ninov, Nucl. Instrum. Methods Phys. Res., Sect. B, Beam Interact. Mater. Atoms 99 (1–4) (1995) 653–656, https://doi.org/10.1016/0168-583X(94)00573-7.

[30] J. Sarén, J. Uusitalo, M. Leino, J. Sorri, Nucl. Instrum. Methods Phys. Res., Sect. A, Accel. Spectrom. Detect. Assoc. Equip. 654 (1) (2011) 508–521, https://doi.org/10.1016/j.nima.2011.06.068.

[31] F.A. Beck, Proceedings of the Workshop Large Gamma-Ray Detector Arrays, Chalk River, Canada, aecl-10613, vol. 2, 1992, p. 364.

[32] C.W. Beausang, S.A. Forbes, P. Fallon, P.J. Nolan, P.J. Twin, J.N. Mo, J.C. Lisle, M.A. Bentley, J. Simpson, F.A. Beck, D. Curien, G. DeFrance, G. Duchêne, D. Popescu, Nucl. Instrum. Methods Phys. Res., Sect. A, Accel. Spectrom. Detect. Assoc. Equip. 313 (1–2) (1992) 37–49, https://doi.org/10.1016/0168-9002(92)90084-H.

[33] C.R. Alvarez, Nucl. Phys. News 3 (3) (1993) 10–13, https://doi.org/10.1080/10506899308221154.

[34] R.D. Page, A.N. Andreyev, D.E. Appelbe, P.A. Butler, S.J. Freeman, P.T. Greenlees, R.-D. Herzberg, D.G. Jenkins, G.D. Jones, P. Jones, D.T. Joss, R. Julin, H. Kettunen, M. Leino, P. Rahkila, P.H. Regan, J. Simpson, J. Uusitalo, S.M. Vincent, R. Wadsworth, Nucl. Instrum. Methods Phys. Res., Sect. B, Beam Interact. Mater. Atoms 204 (2003) 634–637, https://doi.org/10.1016/S0168-583X(02)02143-2.

[35] I. Lazarus, E.E. Appelbe, P.A. Butler, P.J. Coleman-Smith, J.R. Cresswell, S.J. Freeman, R.-D. Herzberg, I. Hibbert, D.T. Joss, S.C. Letts, R.D. Page, V.F.E. Pucknell, P.H. Regan, J. Sampson, J. Simpson, J. Thornhill, R. Wadsworth, IEEE Trans. Nucl. Sci. 48 (3) (2001) 567–569, https://doi.org/10.1109/23.940120.

[36] P. Rahkila, Nucl. Instrum. Methods Phys. Res., Sect. A, Accel. Spectrom. Detect. Assoc. Equip. 595 (3) (2008) 637–642, https://doi.org/10.1016/j.nima.2008.08.039.

[37] D.C. Radford, Nucl. Instrum. Methods Phys., Sect. A 361 (1–2) (1995) 297–305, https://doi.org/10.1016/0168-9002(95)00183-2.

[38] T. Kibédi, T.W. Burrows, M.B. Trzhaskovskaya, P.M. Davidson, C.W. Nestor, Nucl. Instrum. Methods Phys. Res., Sect. A, Accel. Spectrom. Detect. Assoc. Equip. 589 (2) (2008) 202–229, https://doi.org/10.1016/j.nima.2008.02.051.

[39] D.M. Cox, P. Papadakis, A. Briscoe, A. Montes-Plaza, J. Ojala, J. Pakarinen, to be published, 2024.

[40] M. Bender, P. Bonche, T. Duguet, P.-H. Heenen, Phys. Rev. C 69 (2004) 064303, https://doi.org/10.1103/PhysRevC.69.064303.

[41] K. Wrzosek-Lipska, K. Rezynkina, N. Bree, M. Zielińska, L.P. Gaffney, A. Petts, A. Andreyev, B. Bastin, M. Bender, A. Blazhev, B. Bruyneel, P.A. Butler, M.P. Carpenter, J. Cederkäll, E. Clément, T.E. Cocolios, A.N. Deacon, J. Diriken, A. Ekström, C. Fitzpatrick, L.M. Fraile, C. Fransen, S.J. Freeman, J.E. García-Ramos, K. Geibel, R. Gernhäuser, T. Grahn, M. Guttormsen, B. Hadinia, K. Hadyńska-Klęk, M. Hass, P.H. Heenen, R.D. Herzberg, H. Hess, K. Heyde, M. Huyse, O. Ivanov, D.G. Jenkins, R. Julin, N. Kesteloot, T. Kröll, R. Krücken, A.C. Larsen, R. Lutter, P. Marley, P.J. Napiorkowski, R. Orlandi, R.D. Page, J. Pakarinen, N. Patronis, P.J. Peura, E. Piselli, L. Próchniak, P. Rahkila, E. Rapisarda, P. Reiter, A.P. Robinson, M. Scheck, S. Siem, K. Singh Chakkal, J.F. Smith, J. Srebrny, I. Stefanescu, G.M. Tveten, P. Van Duppen, J. Van de Walle, D. Voulot, N. Warr, A. Wiens, J.L. Wood, Eur. Phys. J. A 55 (8) (2019) 130, https://doi.org/10.1140/epja/i2019-12815-2.

[42] ENSDF database as of February 2018.

[43] J. Pakarinen, I.G. Darby, S. Eeckhaudt, T. Enqvist, T. Grahn, P.T. Greenlees, V. Hellemans, K. Heyde, F. Johnston-Theasby, P. Jones, R. Julin, S. Juutinen, H. Kettunen, M. Leino, A.P. Leppänen, P. Nieminen, M. Nyman, R.D. Page, P.M. Raddon, P. Rahkila, C. Scholey, J. Uusitalo, R. Wadsworth, Phys. Rev. C 72 (2005) 011304, https://doi.org/10.1103/PhysRevC.72.011304.

[44] A.M. Oros, K. Heyde, C. De Coster, B. Decroix, R. Wyss, B.R. Barrett, P. Navrátil, Nucl. Phys. A 645 (1) (1999) 107–142, https://doi.org/10.1016/S0375-9474(98)00602-2.

[45] J. Pakarinen, R. Wadsworth, A. Andreyev, S. Eeckhaudt, T. Grahn, P.T. Greenlees, D.G. Jenkins, P. Jones, P. Joshi, R. Julin, S. Juutinen, H. Kettunen, M. Leino, A.-P. Leppänen, P. Nieminen, R.D. Page, J. Perkowski, P. Raddon, P. Rahkila, C. Scholey, J. Uusitalo, K.V.D. Vel, D. Wiseman, pp. 285–292, https://doi.org/10.1142/9789814508865_0038.

[46] D.G. Jenkins, M. Muikku, P.T. Greenlees, K. Hauschild, K. Helariutta, P.M. Jones, R. Julin, S. Juutinen, H. Kankaanpää, N.S. Kelsall, H. Kettunen, P. Kuusiniemi, M. Leino, C.J. Moore, P. Nieminen, C.D. O'Leary, R.D. Page, P. Rakhila, W. Reviol, M.J. Taylor, J. Uusitalo, R. Wadsworth, Phys. Rev. C 62 (2000) 021302, https://doi.org/10.1103/PhysRevC.62.021302.

[47] J.F.C. Cocks, M. Muikku, W. Korten, R. Wadsworth, S. Chmel, J. Domscheit, P.T. Greenlees, K. Helariutta, I. Hibbert, M. Houry, D. Jenkins, P. Jones, R. Julin, S. Juutinen, H. Kankaanpää, H. Kettunen, P. Kuusiniemi, M. Leino, Y. Le Coz, R. Lucas, E. Mergel, R.D. Page, A. Savelius, W. Trzaska, Eur. Phys. J. A 3 (1) (1998) 17–20, https://doi.org/10.1007/s100500050144.

[48] D.G. Popescu, J.C. Waddington, J.A. Cameron, J.K. Johansson, N.C. Schmeing, W. Schmitz, M.P. Carpenter, V.P. Janzen, J. Nyberg, L.L. Riedinger, H. Hübel, G. Kajrys, S. Monaro, S. Pilotte, C. Bourgeois, N. Perrin, H. Sergolle, D. Hojman, A. Korichi, Phys. Rev. C 55 (1997) 1175–1191, https://doi.org/10.1103/PhysRevC.55.1175.

[49] R.R. Chasman, J.L. Egido, L.M. Robledo, Phys. Lett. B 513 (3) (2001) 325–329, https://doi.org/10.1016/S0370-2693(01)00382-3.

[50] R.R. Rodríguez-Guzmán, J.L. Egido, L.M. Robledo, Phys. Rev. C 69 (2004) 054319, https://doi.org/10.1103/PhysRevC.69.054319.

[51] N.A. Smirnova, P.-H. Heenen, G. Neyens, Phys. Lett. B 569 (3) (2003) 151–158, https://doi.org/10.1016/j.physletb.2003.07.042.

[52] J.L. Egido, L.M. Robledo, R.R. Rodríguez-Guzmán, Phys. Rev. Lett. 93 (2004) 082502, https://doi.org/10.1103/PhysRevLett.93.082502.

[53] F.R. May, V.V. Pashkevich, S. Frauendorf, Phys. Lett. B 68 (2) (1977) 113–116, https://doi.org/10.1016/0370-2693(77)90179-4.

[54] J.L. Wood, E.F. Zganjar, C. De Coster, K. Heyde, Nucl. Phys. A 651 (4) (1999) 323–368, https://doi.org/10.1016/S0375-9474(99)00143-8.

[55] A. Montes Plaza, to be published, 2024.

[56] E. Ideguchi, T. Kibédi, J.T.H. Dowie, T.H. Hoang, M. Kumar Raju, N. Aoi, A.J. Mitchell, A.E. Stuchbery, N. Shimizu, Y. Utsuno, A. Akber, L.J. Bignell, B.J. Coombes, T.K. Eriksen, T.J. Gray, G.J. Lane, B.P. McCormick, Phys. Rev. Lett. 128 (2022) 252501, https://doi.org/10.1103/PhysRevLett.128.252501.

[57] P. Papadakis, D.M. Cox, G.G. O'Neill, M.J.G. Borge, P.A. Butler, L.P. Gaffney, P.T. Greenlees, R.-D. Herzberg, A. Illana, D.T. Joss, J. Konki, T. Kröll, J. Ojala, R.D. Page, P. Rahkila, K. Ranttila, J. Thornhill, J. Tuunanen, P. Van Duppen, N. Warr, J. Pakarinen, Eur. Phys. J. A 54 (3) (2018) 42, https://doi.org/10.1140/epja/i2018-12474-9.